Fish CDK2 recruits Dtx4 to degrade TBK1 through ubiquitination in the antiviral response

Long-Feng Lu[a,c], Can Zhang[a,c], Zhuo-Cong Li[a,c], Bao-Jie Cui[a,f], Yang-Yang Wang[a,c], Ke-Jia Han[a,f], Xiao Xu[a,f], Chu-Jing Zhou[a,f], Xiao-Yu Zhou[a,c], Yue Wu[a,c], Na Xu[a,c], Xiao-Li Yang[a,c], Dan-Dan Chen[a,c], Xi-Yin Li[a,c,d,e], Li Zhou[a,c,d,e], Shun Li[a,b,c,d,e 1]

[a]Institute of Hydrobiology, Chinese Academy of Sciences, Wuhan, China

[b]Laboratory for Marine Biology and Biotechnology, Qingdao Marine Science and Technology Center

[c]University of Chinese Academy of Sciences, Beijing, China

[d]State Key Laboratory of Freshwater Ecology and Biotechnology, Institute of Hydrobiology

[e]Key Laboratory of Aquaculture Disease Control, Ministry of Agriculture, Wuhan, China

[f]College of Fisheries and Life Science, Dalian Ocean University, Dalian, China

[1] Corresponding author. Email: bob@ihb.ac.cn

Abstract

Although the classical biological protein cell cycle protein kinase CDK2 has been extensively studied in higher vertebrates, its function in lower vertebrates beyond the regulation of mitosis remains unknown. In this study, we report a distinct mechanism whereby IFN expression is negatively regulated in fish by CDK2. After infection with the spring viremia of carp virus (SVCV), fish CDK2 expression significantly increased in tissues and cells. Moreover, antiviral resistance was improved in *cdk2*$^{-/-}$ homozygotes, and the antiviral cytokine interferon (IFN) expression was significantly higher. At the cellular level, CDK2 overexpression reduced IFN expression, while *cdk2* knockdown increased the ability of cells to produce IFN. Subsequently, it was discovered that fish CDK2 binds and degrades TBK1, resulting in reduced IFN. CDK2 increases the K48-linked ubiquitination of TBK1, causing its degradation, while E3 ubiquitin ligase Dtx4 was found to be involved in this process following the significant enhancement of TBK1 K48-linked ubiquitination. Protein mass spectrometry and immunoblot analysis confirmed that the K567 site on TBK1 is essential for CDK2 to engage with Dtx4 and degrade TBK1; thus, after mutating the K567 site, K48-linked ubiquitination of TBK1 was not enhanced by Dtx4, and TBK1 was not degraded by CDK2. Our data demonstrate that fish CDK2 recruits the E3 ubiquitin ligase Dtx4 to target the K567 site of TBK1 and promote its degradation. These results suggest that CDK2 in lower vertebrates is implicated in a specialized role for antiviral innate immunity.

Introduction

Interferon (IFN) production is central to the host's innate immune response to viral infections. IFN acts as a ligand, binding to receptors on neighboring cell membranes through the autocrine and paracrine pathways, which initiates the Janus kinase/signal transducer and activator of the transcription (JAK/STAT) signaling pathway [1]. This, in turn, leads to the transcription of a large number of antiviral genes, ultimately resulting in the clearance of intracellular viral components [2]. IFN induction depends on cellular pattern recognition receptors (PRRs) and sensing of conserved pathogen-associated molecular patterns (PAMPs), with the retinoic acid-inducible gene I (RIG-I)-like receptors (RLRs) signaling pathway being critical in this system [3]. Viral nucleic acids are recognized by the RLRs, which then initiate a series of signaling events that lead to downstream IFN expression. TANK-binding kinase 1 (TBK1) efficiently phosphorylates IFN regulatory factor 3/7 (IRF3/7), facilitating its nuclear entry [4].

Effective control of IFN production is crucial during viral infection in maintaining immune responses and homeostasis, whereby excessive IFN can cause inflammatory storms that harm the organism. Hence, TBK1 plays a significant role in the IFN signaling pathway and is negatively regulated by various factors to balance IFN expression in the host [5]. Mammalian TBK1 is degraded by NLRP4, which recruits the E3 ubiquitin ligase DTX4 for K48-linked polyubiquitination at Lys670 [6]. Additionally, DYRK2 is crucial in the degradation of TBK1 by NLRP4 through the phosphorylation of Ser527, as mentioned in previous studies [7, 8]. The function of TBK1 is conserved in fish and subject to modulation by multiple molecules to prevent excessive IFN expression. Indeed, TMEM33 in zebrafish serves as a TBK1 substrate, reducing IRF3 phosphorylation and hindering TBK1 kinase activity to diminish IFN expression [9]. Generally, the ability of TBK1 to induce IFN is conserved and tightly regulated within the host.

CDKs are a family of Ser/Thr kinases that act as cell cycle regulators. Cell cycle

progression from the G1 phase to the S phase and from G2 to mitosis is controlled by various cyclin–CDK complexes. For example, CDK2 and cyclin E regulate the G1–S transition [10]. Further studies have unveiled other functions of the CDK family in biological processes beyond cell cycle regulation. The transcription of multiple proinflammatory genes is upregulated in a CDK-dependent fashion throughout the G1 phase [11]. In the context of antitumor immunity in fibrosarcoma and lung carcinoma, inhibiting CDK2 leads to the RB protein being phosphorylated, which results in increased production of type I IFN [12]. Another study demonstrated that inhibiting CDKs or the knockdown of CDKs activities caused a significant blockade in IFN release from culture supernatants [13]. While there are several reported functions of CDKs in innate immunity, understanding the roles of CDKs in this area remains unclear.

The immune systems of higher vertebrates (e.g., humans) and lower vertebrates (e.g., fish) generally exhibit some consistency, although there are notable differences. For instance, IFN phosphorylates fish IRF3, which is only phosphorylated by viruses in mammals. Additionally, fish MVP functions as an IFN-negative regulator, while human MVP mediates IFN-positive expression [14, 15, 16, 17]. There are 13 CDK genes in the human genome and 21 CDK orthologs in zebrafish, indicating that CDK functions are conserved and differ between fish and humans. Our report reveals that fish CDK2 acts as an IFN negative regulator that recruits Dtx4 to facilitate the ubiquitination of TBK1, thereby restricting IFN expression. These findings offer valuable insights into the various roles of CDK2.

Results

1. CDK2 is upregulated during viral infection *in vivo* and *in vitro*

To identify potential molecules linked with viral infection, we generated a transcriptome pool from liver and spleen tissues taken from SVCV-infected zebrafish. Notably, classical cell cycle regulator *cdk2* was among the few upregulated genes in the CDK family (Fig. 1 *A* and *B*). In previous studies, it was found that mammalian

cdk2 was not regulated during viral infection. As shown in Figure 1C, this was confirmed by detecting *cdk2* after THP-1 cells infection with VSV, and it was observed that *cdk2* was not upregulated. Fish *cdk2* was significantly increased upon infection with fish viruses CyHV-2 or SVCV in *Carassius auratus gibelio*, *Danio rerio*, and *Pimephales promelas*, compared to human *cdk2*, indicating that fish CDK2 is involved in the host's antiviral response. Meanwhile, specific qPCR and immunoblot analysis to validate this finding in zebrafish tissues, which demonstrated that the *cdk2* transcript level was significantly increased upon SVCV infection. The CDK2 protein level was also consistently higher in the viral infection group (Fig. 1 *D* and 1 *E*). We investigated whether this CDK2 expression pattern also existed *in vitro*. For this purpose, we used the zebrafish embryonic fibroblast cell line (ZF4) and another cyprinid fish cell line (epithelioma papulosum cyprini (EPC)). During the 48-hour (h) viral infection period, CDK2 was significantly upregulated at the protein level (Fig. 1 *F*). Taken together, the *in vivo* and *in vitro* data suggest that fish CDK2 may play a role in the response to viral infection.

2. *cdk2*$^{-/-}$ fish exhibit effective antiviral capacities

To investigate the role of CDK2 in the antiviral process, we generated a *cdk2* knockout zebrafish homozygote (*cdk2*$^{-/-}$). Our findings demonstrated that the survival rate under viral infection was significantly higher in the *cdk2*$^{-/-}$ group than in the wild-type group (Fig. 2 *A*). We selected the liver, spleen, and kidney as representative tissues in which to analyze the *cdk2*$^{-/-}$ antiviral capacity. In the H&E staining assay, severe tissue damage was observed in the wild-type group, while the *cdk2*$^{-/-}$ group displayed dramatically less tissue damage (Fig. 2 *B*). The viral transcripts in these tissues were observed and then compared to the abundance in the wild-type. The replication of viral genes, such as SVCV N, was typically inhibited in *cdk2*$^{-/-}$ homozygote tissues (Fig. 2 *C*). Viral protein level analysis also confirmed these results, as SVCV G, N, and P proteins were suppressed in *cdk2*$^{-/-}$ homozygotes (Fig. 2 *D*).

Transcriptomics analysis was employed to investigate the antiviral regulation by

CDK2. Differential expression analysis identified 1707 upregulated genes and 1490 downregulated genes in the liver of *cdk2* knockout zebrafish versus WT zebrafish after SVCV infection (Fig. 2 *E*). Moreover, gene set enrichment analyses (GSEAs) were performed to analyze the IFN response to virus infection-related genes, which demonstrated that these genes were significantly activated in the *cdk2*$^{-/-}$ group (Fig. 2 *F*). Differential expression analysis further showed that *cdk2* knockout results in the upregulation of many IFN-stimulated genes (ISGs) after SVCV infection (Fig. 2 *G*). To procure the transcriptome data, IFN was assayed in zebrafish tissues, including liver, spleen, and kidney. Similar to in the transcriptome assay, IFN was found to be significantly higher in the *cdk2*$^{-/-}$ groups, indicating that stronger antiviral capacity and higher IFN transcription occurred in *cdk2*$^{-/-}$ fish (Fig. 2 *H*). Collectively, these data suggest that viral replication was hindered in the *cdk2*$^{-/-}$ fish.

3. CDK2 inhibits IFN expression and promotes viral proliferation

The impact of CDK2 on viral infection was examined in relation to IFN. The IFN response is an essential mechanism for host resistance against viruses. Overexpression of CDK2 decreased the IFN promoter and ISRE motif activation by SVCV or poly I:C (Fig. 3 *A*). An effective shcdk2 was produced and identified (Fig. 3 *B*). The impact of CDK2 knockdown was explored, with the results suggesting that the downregulation of CDK2 facilitates IFN promoter activity (Fig. 3 *C*). The mRNA levels of *ifn* and downstream ISG *vig1* transcription were monitored, revealing that CDK2 caused a significant decrease in *ifn* and *vig1*, whereas the knockdown of CDK2 increased the IFN response (Fig. 3 *D*). In the antiviral capacity assays, CDK2 from zebrafish, gibel carp, and grass carp all promoted the proliferation of their respective corresponding viruses (Fig. 3 *E*). Conversely, CDK2 knockdown significantly suppressed viral proliferation (Fig. 3 *F*). Cells overexpressing CDK2 showed enhanced production of viral mRNA and proteins, while CDK2-knockdown cells showed attenuation of the same viral mRNA and proteins (Fig. 3 *G* and *H*). Immunofluorescence revealed a higher intensity of green signals indicating SVCV N protein in the CDK2 overexpression group compared to the control, while a lower

green signal was observed in the CDK2-knockdown group compared to the normal group (Fig. 3 *I*). These findings suggest that CDK2 inhibits IFN expression in the host and reduces antiviral capacity.

4. CDK2 interacts with TBK1 and reduces its expression

The RLR pathway plays an important role in IFN activation. To investigate whether CDK2 counters RLR signaling, as observed earlier, we examined whether CDK2 inhibits RLR factors that activate IFN promoters. The activation of the IFN promoters induced by MAVS and TBK1 was significantly inhibited by CDK2, whereas it was unaffected by MITA (Fig. 4 *A*). CDK2 knockdown restored MAVS and TBK1 functions following IFN promoter stimulation (Fig. 4 *B*). Moreover, the *ifn* and *vig1* transcripts were monitored. The results showed that CDK2 notably reduced *ifn* and *vig1* mRNA levels, whereas the CDK2 knockdown improved the IFN response (Fig. 4 *C* and *D*). These findings suggest that CDK2 targets either MAVS or TBK1. The subcellular localization of CDK2 was observed to be distributed throughout the cell. However, TBK1 and MAVS exhibited cytoplasmic localization, while there appeared to be a significant punctate overlap between CDK2 and TBK1, indicating a possible association between CDK2 and TBK1 (Fig. 4 *E*). Subsequently, association analysis of CDK2 and MAVS or TBK1 was conducted. The co-IP assay revealed an interaction between CDK2 and TBK1, yet not between CDK2 and MAVS (Fig. 4 *F*). Afterward, an endogenous co-IP assay was performed to confirm the interaction between CDK2 and TBK1, while the interaction was also verified with TBK1 or CDK2 being enriched (Fig. 4 *G*). To identify the essential domain that mediates the interaction with CDK2, two truncated TBK1 mutants were generated (Fig. 4 *H*). The TBK1-ΔN-flag, which lacked the kinase domain, meaning it cannot bind to CDK2, indicated that the kinase domain in TBK1 is necessary for it to associate with CDK2 (Fig. 4 *I*). Since the interaction between CDK2 and TBK1 was confirmed, whether CDK2 affects TBK1 stability was also investigated. Co-overexpression of the relevant RLR factors and CDK2 demonstrated that TBK1 expression was substantially decreased in the presence of CDK2, compared to MAVS (Fig. 4 *J*). Consistently,

CDK2 impaired endogenous TBK1 under both normal and stimulation states, whereas CDK2 knockdown abolished this effect, indicating that CDK2 impaired TBK1 expression (Fig. 4 *K* and *L*). The expression of TBK1 was also significantly increased in the liver, spleen, and kidney of *cdk2*$^{-/-}$ fish, confirming the *in vivo* impact of CDK2 on TBK1 expression (Fig. 4 *M*). Subsequently, its biological function was studied to investigate whether CDK2 affects the crucial antiviral role of TBK1. During SVCV infection, cells overexpressing TBK1 showed little CPE; however, CDK2 dramatically counteracted the antiviral capacity of TBK1, as confirmed by virus titer identification (Fig. 4 *N*). For viral protein expression, CDK2 restored the TBK1-mediated prevention of viral protein expression, including SVCV G, N, and P proteins. Immunofluorescence also demonstrated that the inhibition of SVCV N protein by TBK1 was restored following CDK2 overexpression (Fig. 4 *O* and *P*). CDK2 also restored viral nucleic acid transcription, which was abolished by TBK1 (Fig. 4 *Q*). These results demonstrate that CDK2 interacts with the kinase domain in TBK1, leading to reduced expression and a weakened antiviral effect.

5. CDK2 causes TBK1 degradation by increasing K48-linked polyubiquitination

The next step was to investigate the mechanisms through which CDK2 negatively regulates TBK1. To determine whether the decrease in TBK1 occurred at the mRNA or protein level, *tbk1* transcription was monitored. CDK2 had little effect on *tbk1* in either the control or virus-infected groups (Fig. 5 *A*). Therefore, attention was placed on modulating TBK1 at the protein level. Various reagents that inhibit the ubiquitin (Ub)-proteasome and autophagosome, such as MG132, 3-MA, Baf-A1, and CQ, were utilized to clarify the precise regulatory mechanism. Compared to the autophagosome inhibitors 3-MA, Baf-A1, and CQ, using the Ub-proteasome inhibitor MG132 significantly impeded TBK1 degradation in a dose-dependent manner (Fig. 5 *B* and *C*). This suggests that the degradation of TBK1 by CDK2 is proteasome-dependent. Similar results were observed for endogenous TBK1 in the presence or absence of poly I:C stimulation or SVCV infection (Fig. 5 *D*). Since ubiquitination is an important process during proteasome-dependent degradation, we

next investigated whether ubiquitination was important in the CDK2-mediated degradation of TBK1. Expectedly, immunoblot analysis confirmed that CDK2 increased the ubiquitination of TBK1 (Fig. 5 *E*). Polyubiquitin chain modification, either K48-linked or K63-linked, can either target proteins for degradation or increase stability. To investigate how TBK1 was modified, we performed MS analysis of ubiquitinated TBK1 from cells and found that K48-linked polyubiquitinated TBK1 was readily detected in CDK2-overexpressed cells, whereas K63-linked polyubiquitinated TBK1 was hardly detected (Fig. 5 *F*). Consistently, when we transfected EPC cells with TBK1-Myc, CDK2-HA, WT-Ub, K48-Ub, or K63-Ub, we found that CDK2 markedly increased K48-linked, but not K63-linked, ubiquitination of TBK1, while CDK2 knockdown remarkably attenuated K48-linked ubiquitination of TBK1 (Fig. 5 *G* and *H*). Taken together, these findings indicate that the CDK2 triggers the degradation of TBK1 through K48-linked ubiquitination.

6. CDK2 recruits the ubiquitin E3 ligase Dtx4 to interact with and degrade TBK1

Since CDK2 is not an E3 ubiquitin ligase, it is speculated that CDK2-mediated degradation of TBK1 does not occur directly; instead, CDK2 acts as an adaptor to recruit an E3 ubiquitin ligase to TBK1. Several homologs of TBK1-associated E3 ubiquitin ligases in mammals were cloned into fish to detect protein interactions. It was found that Trim11 and Dtx4 are associated with TBK1, and these interactions were verified through inverse experiments (Fig. 6 *A and B*). Moreover, protein interactions between CDK2 and Trim11 or Dtx4 were investigated. Dtx4 exhibited a significant interaction with CDK2 but not with Trim11, indicating that Dtx4 interacts with both TBK1 and CDK2 (Fig. 6 *C*). Hence, Dtx4 was the main focus of the subsequent assays. Since Dtx4 is a potential ubiquitin ligase for TBK1, we verified whether CDK2 facilitated the interaction between Dtx4 and TBK1. Overexpression of CDK2 significantly increased the interaction between Dtx4 and TBK1, while CDK2 knockdown impeded this progress, suggesting that CDK2 promotes the interaction between Dtx4 and TBK1 (Fig. 6 *D*). Next, the impact of the Dtx4 interaction was

elucidated. Overexpression of DTX4 amplified CDK2-mediated inhibition of IFN promoter activity induced by TBK1 (Fig. 6 *E*). Moreover, CDK2-mediated reduction of *ifn* and *vig1* mRNAs activated by TBK1 was also augmented by Dtx4 overexpression (Fig. 6 *F*). In contrast to the normal state where CDK2 degrades TBK1, Dtx4 overexpression increased degradation (Fig. 6 *G*). The degradation of endogenous TBK1 by CDK2 was more severe when Dtx4 was overexpressed (Fig. 6 *H*). Two shRNAs were designed and generated, and after validation of exogenous and endogenous knockdown efficiencies, sh*dtx4*#1 was selected for the following assay (Fig. 6 *I*). Dtx4 knockdown remarkably abrogated CDK2 suppression of TBK1-induced IFN promoter activity and *ifn* and *vig1* mRNAs, and CDK2 regulated both the exogenous and endogenous degradation of TBK1 (Fig. 6 *J–M*). Overall, CDK2 recruits the E3 ubiquitin ligase Dtx4 to degrade TBK1.

7. The K567 site in TBK1 plays an essential role in CDK2-mediated degradation

By accelerating CDK2-mediated TBK1 degradation, the precise ubiquitin ligase function of Dtx4 was identified. Compared to Trim11, Dtx4 significantly enhanced the CDK2-potentiated ubiquitination of TBK1 (Fig. 7 *A*). Further analysis revealed that Dtx4 overexpression augmented K48-linked TBK1 ubiquitination and that Dtx4 knockdown reduced this ubiquitination. Thus, demonstrating that Dtx4 is critical for CDK2-mediated TBK1 ubiquitination (Fig. 7 *B* and *C*). To analyze the molecular mechanism of TBK1 modification by ubiquitination, two potential TBK1 lysine sites, namely K154 and K567, were identified for modification by ubiquitination using mass spectrometry analysis (Fig. 7 *D*). Subsequently, two TBK1 mutants were generated with point mutations by mutating K154 and K567 to R to create K154R and K567R. In the ubiquitination assay, TBK1-K567R could not be ubiquitinated by CDK2, while K154R was almost identical to the wild-type TBK1 (Fig. 7 *E*). This result was also characterized in the K48-linked ubiquitination assay (Fig. 7 *F*). Moreover, Dtx4 significantly increased CDK2-mediated TBK1 wild-type and K48-linked ubiquitination but failed to enhance these processes in the K567R mutant group of TBK1 (Fig. 7 *G* and *H*). This strongly suggests that K567 is a crucial site for

TBK1 ubiquitination by Dtx4. Additionally, when TBK1-K567 was mutated, CDK2-mediated degradation of TBK1 failed, and the IFN induction and antiviral capacity restriction of TBK1 by CDK2 was also ineffective (Fig. 7 *I–O*). These findings confirm the essential role of TBK1-K567 in recruiting Dtx4 through CDK2. The RING domain is crucial for E3 ubiquitin ligase activity. Three truncated mutants of Dtx4 were generated (Fig. 7 *P*). The mutant lacking the RING domain (Dtx4-△RING) significantly impaired the interaction between Dtx4 and TBK1 or CDK2 (Fig. 7 *Q*). In the ubiquitination assay, the wild-type Dtx4 enhanced TBK1 and K48-linked ubiquitination. On the other hand, Dtx4-△RING failed, indicating that the RING domain was necessary for TBK1 ubiquitination by Dtx4 (Fig. 7 *R*). In summary, the data above demonstrates that the K567 site in TBK1 and the RING domain in the E3 ubiquitin ligase Dtx4 are crucial for CDK2 ubiquitination, leading to the degradation of TBK1.

Discussion

Although IFN responses exhibit powerful functions in defending against viral infection, excessive activation of IFN production may cause autoimmune disease. Therefore, the host needs to develop a set of regulatory mechanisms to balance immune responses. In this study, we illustrated a novel role for fish CDK2 in the negative regulation of IFN expression, which degraded TBK1 for K48-linked ubiquitination by recruiting E3 ubiquitin ligase Dtx4.

TBK1 is a central kinase in MAVS, STING, and TIR-domain-containing adapter-inducing IFN-β (TRIF) signaling complexes, which promote the phosphorylation of IRF3 and the production of IFN. Thus, the activation of TBK1 must be tightly regulated to avoid excessive autoimmune responses. TBK1 activity can be regulated in various ways, including phosphorylation, ubiquitination, SUMOylation, and preventing the formation of functional TBK1-containing complexes. For instance, receptor tyrosine kinase HER2 recruits AKT1 to directly phosphorylate TBK1, which disrupts the TBK1–STING association and K63-linked

ubiquitination of TBK1, thus, suppressing antiviral responses [18]. Siglec1 associates with DAP12 and SHP2 to recruit the E3 ubiquitin ligase TRIM27, which induces K48-linked-ubiquitination-mediated TBK1 degradation, resulting in the inhibition of IFN production [19]. Similar to in mammals, TBK1 also dramatically activates the IFN signaling pathway in fish. Therefore, its activation must be precisely modulated. For example, cytokine receptor-like factor 3 (Crlf3) promotes the degradation of TBK1 via K48-linked ubiquitination, resulting in inhibition of IFN production [20]. While TBK1 regulation has received attention, multiple molecules and underlying molecular mechanisms have not been fully characterized as potential TBK1 targets.

Ubiquitination is one of the most versatile post-translational modifications (PTMs) of proteins and plays numerous vital roles in regulating antiviral responses. Ubiquitin comprises seven lysine residues (K6, K11, K27, K29, K33, K48, and K63); thus, seven different polyubiquitin chains can be produced [21]. K48-linked polyubiquitination is used to signal for proteasomal degradation of substrate proteins. In contrast, K63-linked polyubiquitination is a non-proteolytic mode of modification that plays several vital roles in stabilizing and activating target proteins [22]. Multiple studies have shown that different polyubiquitin chains can regulate the expression and activation of TBK1 [5]. For instance, Nrdp1, MIB1/2, RNF128, and NLRC4 mediate the K63□linked polyubiquitination of TBK1 and facilitate its activation [23, 24, 25, 26]. TRIP, SOCS3, and TRAF3IP3 have been proven to negatively regulate the IFN signaling pathway by targeting TBK1 for K48-linked polyubiquitination and degradation [27, 28, 29]. Ubiquitination modification is a tightly regulated and reversible process that maintains cellular homeostasis. For example, the deubiquitinating enzymes CYLD, RNF114B, USP2b, and UBE2S remove the K63-linked polyubiquitination of TBK1 to block its activation [30, 31, 32, 33]. Additionally, the USP1–UAF1 deubiquitinate complex has been found to cleave the K48□linked polyubiquitination of TBK1 to reverse its degradation process [34]. These findings are specific to the ubiquitination of mammalian TBK1. Although fish TBK1 is highly conserved compared to mammalian TBK1, its ubiquitination modifications are worth exploring. Our study identified a previously unrecognized role for CDK2 in

357 promoting the K48□linked polyubiquitination and proteasomal degradation of fish
358 TBK1.

359 A series of ubiquitin-related enzymes are responsible for ubiquitination,
360 including ubiquitin-activating enzymes (E1s), ubiquitin-conjugating enzymes (E2s),
361 and ubiquitin ligases (E3s). Among them, the E3s are the critical components that
362 determine the substrate specificity [35]. E3s are generally divided into two large classes,
363 including the homology to the E6-associated protein carboxyl terminus (HECT)
364 domain-containing E3 ligases and the really interesting new gene (RING)
365 domain-containing E3 ligases [36]. Multiple studies have demonstrated that E3 ligases,
366 including TRIP, Socs3, Dtx4, and TRIM27, specifically target TBK1 for K48-linked
367 polyubiquitination and degradation [19, 27, 28, 37]. However, CDK2 is not an E3 ubiquitin
368 ligase. Thus, we reasoned that CDK2 might be a mediator in the recruitment of an E3
369 ubiquitin ligase for K48-linked polyubiquitination. To validate this hypothesis, we
370 investigated and screened hTBK1-associated E3 ubiquitin ligases, demonstrating that
371 Dtx4 interacted with CDK2 and enhanced the K48-linked polyubiquitination of TBK1.
372 Meanwhile, our results showed that the RING domain in Dtx4 was necessary for
373 modifying TBK1 through ubiquitination.

374 Recent studies have demonstrated that CDK activity is crucial for virus-induced
375 innate immune responses [38]. Reports indicate that CDKs are involved in the Toll-like
376 receptor (TLR) signaling pathway, the nuclear factor-κB (NF-κB) signaling pathway,
377 and the JAK-STAT signaling pathway. For instance, CDK8 and/or CDK19 enhanced
378 the transcription of inflammatory genes, such as IL-8 and IL-10, in cells following
379 TLR9 stimulation [39]. CDKs and NF-κB establish a remarkable paradigm where CDKs
380 can act directly on substrate proteins rather than depending solely on transcriptional
381 control [40]. It has been reported that CDK1 serves as a positive regulator of the IFN-I
382 signaling pathway, facilitating STAT1 phosphorylation, which subsequently boosts the
383 expression of ISGs [41]. Furthermore, inhibiting CDK activity has been shown to
384 obstruct STAT phosphorylation, proinflammatory gene activation, and ISG mRNA
385 induction in response to SeV infection [42]. It is important to note that no evidence
386 suggests the involvement of CDKs in RLR signaling pathways. This study has shown

that fish CDK2 functions as a negative regulator of the key kinase TBK1, which is involved in the RLR signaling pathway. Variations in CDK2 activity during different phases of the cell cycle may lead to changes in the expression and function of TBK1. Our findings suggest that heightened CDK2 activity may suppress TBK1 expression, thereby hindering the cell's capacity to produce IFN. Conversely, during the late phase of the cell cycle or in an inhibited state, TBK1 expression may rise, enhancing IFN synthesis and release. In summary, CDK2 is involved in intracellular signaling by modulating TBK1 levels and IFN production, affecting the cellular immune response and cycle regulation—two processes that are notably distinct at various stages of the cell cycle. A better understanding of the relationship between CDK2 and RLR signaling pathways will enhance our grasp of the regulatory mechanisms of CDKs in antiviral innate immunity. In addition, we now briefly propose a model wherein CDK2 activity during the S phase may suppress TBK1-mediated IFN production to allow viral replication, while CDK2 inhibition (e.g., in G1) may enhance IFN responses. This hypothesis will be the subject of our future work, including cell cycle synchronization experiments and time-course analyses of CDK2 activity and IFN output during infection.

CDK2 is a multifunctional kinase involved in many critical cellular processes, including cell cycle progression, differentiation, cancer, immunity, etc. [43]. To date, there has been limited research conducted on fish CDK2 in the regulation of cell cycle progression. The details are as follows: It has been reported that the kinase activity of goldfish CDK2 significantly increases during oocyte maturation [44]. Furthermore, UHRF1 phosphorylation by cyclin A2/CDK2 is crucial for zebrafish embryogenesis [45]. Additionally, a novel CDK2 homolog has been identified in Japanese lamprey, which plays a crucial role in apoptosis [46]. Red grouper nervous necrosis virus (RGNNV) infection activates the p53 pathway, leading to the upregulation of p21 and downregulation of cyclin E and CDK2, which forces infected cells to remain in the G1/S replicative phase [47]. In addition, we selected representative species from each of the six major vertebrate groups and compared their CDK2 protein sequences, discovering that they are over 90% similar to one another. This suggests that the

function of CDK2 may be conserved to some extent across vertebrates. Furthermore, CDK2 inhibition has been shown to enhance anti-tumor immunity by increasing the IFN response to endogenous retroviruses [12]. Here, we reveal the role of CDK2 in modulating the RLR signaling pathway during innate immunity. Upon infection with SVCV, CDK2 expression was induced. However, the precise upstream signaling pathways that regulate CDK2 during viral infection remain to be fully elucidated. It is hypothesized that viral RNA sensors may activate transcription factors that bind to the cdk2 promoter; however, further investigation is required to confirm this. CDK2 deficiency or knockdown enhanced the antiviral response both *in vitro* and *in vivo*, while CDK2 overexpression promoted viral replication. Thus, our study identifies CDK2 as a negative regulator of antiviral immune responses in addition to its well-studied function in cell cycle regulation. Meanwhile, the E3 ubiquitin ligase Dtx4 is also required to regulate antiviral immune responses. Furthermore, evidence is presented demonstrating that CDK2 enhances the interaction between Dtx4 and TBK1, thus suggesting that CDK2 functions as a scaffold protein to facilitate the formation of a ternary complex. However, further study is required to ascertain the precise structural basis of this interaction, including whether CDK2's kinase activity is required.

In conclusion, our results identified a novel function of CDK2 in the negative regulation of TBK1-mediated IFN production. CDK2 interacted with TBK1 and recruited the E3 ubiquitin ligase Dtx4 to facilitate the K48□linked polyubiquitination at Lys567 residues in TBK1, eventually leading to the proteasomal degradation of TBK1. Our findings have revealed a previously unrecognized role for CDK2 in regulating immune homeostasis, providing molecular insight into the mechanisms through which CDK2–DTX4 targets TBK1 for ubiquitination and degradation.

Methods

Ethics statement

The experiments involved in this study were conducted in compliance with

ethical regulations. The fish experiments were carried out under the guidance of the European Union Guidelines for the Handling of Laboratory Animals (2010/63/EU) and approved by the Ethics Committee for Animal Experiments of the Institute of Aquatic Biology of the Chinese Academy of Sciences (No. 2023-068).

Fish, cells, and viruses

Mature zebrafish individuals 2.5 months after hatching (0.4 ± 0.1 g) were selected in this study. AB line wild-type zebrafish (Danio rerio) and cdk2 mutant zebrafish (CZ1442: *cdk2*$^{ihb488/+}$) were obtained from the China National Zebrafish Resource Center (CZRC) and bred using standardized procedures. In accordance with ethical requirements and national animal welfare guidelines, all experimental fish were required to undergo a two-week acclimatization period in the laboratory and have their health assessed prior to the study. Only fish that appeared healthy and were mobile were used for scientific research. ZF4 cells (American Type Culture Collection, ATCC) were cultured in Ham's F-12 medium (Invitrogen) supplemented with 10% fetal bovine serum (FBS) at 28 ˚C and 5% CO_2. EPC cells and ctenopharyngodon idellus kidney (CIK) cells were obtained from the Chinese Culture Collection Centre for Type Cultures (CCTCC), Gibel carp brain (GiCB) cells were provided by Ling-Bing Zeng (Yangtze River Fisheries Research Institute, Chinese Academy of Fishery Sciences), these cells were maintained at 28°C in 5% CO_2 in medium 199 (Invitrogen) supplemented with 10% FBS. THP1 cells originally obtained from ATCC were maintained in RPMI 1640 medium supplemented with 10% FBS. SVCV was propagated in EPC cells until a cytopathogenic effect (CPE) was observed, and then cell culture fluid containing SVCV was harvested and centrifuged at 4×10^3 *g* for 20 min to remove the cell debris, and the supernatant was stored at -80°C until used. GCRV (strain 873, group □) and vesicular stomatitis virus (VSV) was provided by Prof. Wuhan Xiao (Institute of Hydrobiology, Chinese Academy of Sciences). GCRV was propagated in CIK cells and harvested in a similar way to SVCV. Cyprinid herpesvirus 2 (CyHV2, obtained from Yancheng city, Jiangsu province, China) was provided by Prof. Liqun Lu (Shanghai Ocean University). CyHV-2 was propagated in GICB cells and harvested in a similar way to SVCV.

476 **Plasmid construction and reagents**

477 The sequence of zebrafish CDK2 (GenBank accession number: NM_213406.1)
478 was obtained from the National Centre for Biotechnology Information (NCBI)
479 website. CDK2 was amplified by polymerase chain reaction (PCR) using cDNA from
480 adult zebrafish tissues as a template and cloned into the expression vector pCMV-HA
481 or pCMV-Myc (Clontech) vectors. Zebrafish MAVS (NM_001080584.2), TBK1
482 (NM_001044748.2) and the truncated mutants of TBK1, Dtx4 (XM_002660524.5)
483 and the truncated mutants of Dtx4, Trim11 (XM_021470074.1), Traip
484 (NM_205607.1), Socs3a (NM_199950.1), and GAPDH (NM_001115114.1) were
485 cloned into pCMV-Myc and pCMV-Tag2C vectors. The short hairpin RNA of
486 Pimephales promelas CDK2 (XM_039663387.1) and Dtx4 (XM_039689084.1) were
487 designed by BLOCK-iT RNAi Designer and cloned into the pLKO.1-TRC Cloning
488 vector. For subcellular localization experiments, CDK2 was constructed onto
489 pEGFP-N3 (Clontech), while MAVS and TBK1 were constructed onto
490 pCS2-mCherry (Clontech). The plasmids containing zebrafish IFNφ1pro-Luc and
491 ISRE-Luc in the pGL3-Basic luciferase reporter vector (Promega) were constructed as
492 described previously. The *Renilla* luciferase internal control vector (pRL-TK) was
493 purchased from Promega. The ubiquitin mutant expression plasmids Lys-48 and
494 Lys-63 (all lysine residues were mutated except Lys-48 or Lys-63) were ligated into
495 the pCMV-HA vectors named Ub-K48O-HA and Ub-K63O-HA. All constructs were
496 confirmed by DNA sequencing. Polyinosinic-polycytidylic acid (poly I:C) was
497 purchased from Sigma-Aldrich used at a final concentration of 1 μg/μl. MG132 (Cat.
498 No. M7449), 3-Methyladenine (3-MA) (Cat. No. M9281), Chloroquine (CQ) (Cat. No.
499 C6628) were obtained from Sigma-Aldrich. Bafilomycin A1 (Baf-A1) (Cat. No.
500 S1413) was obtained from Selleck.

501 **Transcriptomic analysis**

502 Total RNA was extracted using the TRIzol method and assessed for RNA purity
503 and quantification using a NanoDrop 2000 spectrophotometer (Thermo Scientific,
504 Waltham, U.S.A.), and RNA integrity was assessed using an Agilent 2100
505 Bioanalyzer (Agilent Technologies, Santa Clara, U.S.A.). Santa Clara, U.S.A).

Transcriptome sequencing and data analysis were performed by OE Biotech (Shanghai, China). The raw sequencing data was submitted to the NGDC (National Genomics Data Center) (GSA accession number: CRA008409).

Transient transfection and virus infection

EPC cells were transfected in 6-well and 24-well plates using transfection reagents from FishTrans (MeiSenTe Biotechnology) according to the manufacturer's protocol. Antiviral assays were performed in 24-well plates by transfecting EPC cells with the plasmids shown in the figure. At 24 h post-transfection, cells were infected with SVCV at a multiplicity of infection (MOI = 0.001), GCRV (MOI = 0.001), CyHV-2 (MOI = 0.1). After 48 h or 72 h, supernatant aliquots were harvested for detection of virus titers, the cell monolayers were fixed by 4% paraformaldehyde (PFA) and stained with 1% crystal violet for visualizing CPE. For virus titration, 200 μl of culture medium were collected at 48 h post-infection and used for detection of virus titers according to the method of Reed and Muench. The supernatants were subjected to 3-fold or 10-fold serial dilutions and then added (100 μl) onto a monolayer of EPC cells cultured in a 96-well plate. After 48 or 72 h, the medium was removed and the cells were washed with PBS, fixed by 4% PFA and stained with 1% crystal violet. The virus titer was expressed as 50% tissue culture infective dose ($TCID_{50}$/ml). For viral infection, fish were anesthetized with methanesulfonate (MS-222) and intraperitoneally (i.p.) injected with 5 μl of M199 containing SVCV (5×10^8 $TCID_{50}$/ml). The i.p. injection of PBS was used as mock infection. Then the fish were migrated into the aquarium containing new aquatic water.

Luciferase activity assay

EPC cells were cultured overnight in 24-well plates and then co-transfected with the expression plasmid and luciferase reporter plasmid. The cells were infected with SVCV or transfected with poly I:C for 24 h prior to harvest. To ensure that the same total amount of DNA was transfected in each well, pCMV-HA empty vector was used. At 24 h post-stimulation, cells were washed with phosphate-buffered saline (PBS) and lysed for measuring luciferase activity by the Dual-Luciferase Reporter Assay System (Promega) according to the manufacturer's instructions. Firefly luciferase activity was

normalized based on the Renilla luciferase activity.

RNA extraction, reverse transcription, and quantitative PCR (qPCR)

The RNA was extracted using TRIzol reagent (Invitrogen), and first-strand cDNA was synthesized with a PrimeScript RT kit with gDNA Eraser (Takara). qPCR was performed on the CFX96 Real-Time System (Bio-Rad) using SYBR green PCR Master Mix (Yeasen). PCR conditions were as follows: 95°C for 5 min and then 40 cycles of 95°C for 20 s, 60°C for 20 s, and 72°C for 20 s. All primers used for qPCRs are shown in Table S1, and *β-actin* gene was used as an internal control. The relative fold changes were calculated by comparison to the corresponding controls using the $2^{-\Delta\Delta Ct}$ method (where CT was the threshold cycle).

Co-immunoprecipitation (Co-IP) assay

EPC cells were cultured in 10 cm^2 dishes overnight and transfected with 10 μg of plasmid, as shown. At 24 h post-transfection, the medium was discarded, and the cells were washed with PBS. Then the cells were lysed in 1 ml of radioimmunoprecipitation (RIPA) lysis buffer [1% NP-40, 50 mM Tris-HCl, pH 7.5, 150 mM NaCl, 1 mM EDTA, 1 mM NaF, 1 mM sodium orthovanadate (Na_3VO_4), 1 mM phenyl-methylsulfonyl fluoride (PMSF), 0.25% sodium deoxycholate] containing protease inhibitor cocktail (Sigma-Aldrich) at 4°C for 1 h on a rocker platform. The cellular debris was removed by centrifugation at 12,000 × *g* for 15 min at 4°C. The supernatant was transferred to a fresh tube and incubated with 20 μl anti-Flag/HA/Myc affinity gel (Sigma-Aldrich) overnight at 4°C with constant rotating incubation. These samples were further analyzed by immunoblotting (IB). Immunoprecipitated proteins were collected by centrifugation at 5000 × *g* for 1 min at 4°C, washed three times with lysis buffer and resuspended in 50 μl 2 × SDS sample buffer. The immunoprecipitates and whole cell lysates (WCLs) were analyzed by IB with the indicated antibodies (Abs).

In vivo ubiquitination assay

Transfected EPC cells were washed twice with 10 mL ice-cold PBS and then digested with 1 mL 0.25% trypsin-EDTA (1×) (Invitrogen) for 2–3 min until the cells were dislodged. 100 μL FBS was added to neutralize the trypsin and the cells were

resuspended into 1.5 mL centrifuge tube, centrifuged at 2000 ×*g* for 5 min. The supernatant was discarded and the cell precipitations were resuspended using 1 mL PBS and centrifuged at 2000 ×*g* for 5 min. The collected cell precipitations were lysed using 100 μL PBS containing 1% SDS and denatured by heating for 10 min. The supernatants were diluted with lysis buffer until the concentration of SDS was decreased to 0.1%. The diluted supernatants were incubated with 20 μL anti-Myc affinity gel overnight at 4°C with constant agitation. These samples were further analyzed by IB. Immunoprecipitated proteins were collected by centrifugation at 5000 ×*g* for 1 min at 4°C, washed for three times with lysis buffer and resuspended in 100 μL 1× SDS sample buffer.

Immunoblot analysis

Immunoprecipitates or WCLs were analyzed as described previously. Antibodies were diluted as follows: anti-β-actin (ABclonal, AC026) at 1:3000, anti-Flag (Sigma-Aldrich, F1804) at 1:3000, anti-HA (Covance, MMS-101R) at 1:3000, anti-Myc (Santa Cruz Biotechnology, sc-40) at 1:3000, anti-Dtx4 (Thermo Scientific, PA5-46146) at 1:1000, anti-CDK2 (GeneTex, GTX101226) at 1:1000, and HRP-conjugated anti-mouse/rabbit IgG (Thermo Scientific, 31430/31460) at 1:5000, anti-N/P/G/TBK1/CDK2 (prepared and purified in our lab) at 1:2000.

Immunofluorescence (IF)

EPC cells were plated onto glass coverslips in 6-well plates and infected with SVCV (MOI = 1) 24 h. Then the cells were washed with PBS and fixed in 4% PFA at room temperature for 1 h and permeabilized with 0.2% Triton X-100 in ice-cold PBS for 15 min. The samples were blocked for 1 h at room temperature in PBS containing 2% bovine serum albumin (BSA, Sigma-Aldrich). After additional PBS washing, the samples were incubated with anti-N Ab in PBS containing 2% BSA for 2-4 h at room temperature. After three times washed by PBS, the samples were incubated with secondary Ab (Alexa Fluor 488 AffiniPure Donkey anti-Rabbit IgG (H+L) (34206ES60, 1:10,000) in PBS containing 2% BSA for 1 h at room temperature. After additional PBS washing, the cells were finally stained with 1 μg/ml 4′, 6-diamidino-2-phenylindole (DAPI; Beyotime Institute of Biotechnology, Shanghai,

China) for 10 min in the dark at room temperature. Finally, the coverslips were washed and observed with a confocal microscope under a 10× immersion objective (SP8; Leica).

Fluorescent microscopy

EPC cells were plated onto coverslips in 6-well plates and transfected with the plasmids indicated for 24 h. Then the cells were washed twice with PBS and fixed with 4% PFA for 1 h. After being washed three times with PBS, the cells were stained with 1 μg/ml DAPI for 15 min in the dark at room temperature. Finally, the coverslips were washed and observed with a confocal microscope under a 63× oil immersion objective (SP8; Leica).

Histopathology

Liver, spleen, and kidney tissues from three individuals of control or virus-infected fish at 2 days post infection (dpi) were dissected, and fixed in 10% phosphate-buffered formalin overnight. Then the samples were dehydrated in ascending grades of alcohol and embedded into paraffin. Sections at 5 μm thickness were taken and stained with hematoxylin and eosin (H&E). Histological changes were examined by optical microscopy at ×40 magnification and were analyzed by the Aperio ImageScope software.

Statistics analysis

For fish survival analysis, Kaplan-Meier survival curves were generated and analyzed by Log-rank test. For the bar graph, one representative experiment of at least three independent experiments is shown, and each was done in triplicate. For the dot plot graph, each dot point represents one independent biological replicate. Unpaired Student's t test was used for statistical analysis. Data are expressed as mean ± standard error of the mean (SEM). A p value < 0.05 was considered statistically significant.

Acknowledgments

We thank Fang Zhou (Institute of Hydrobiology, Chinese Academy of Sciences) for assistance with confocal microscopy analysis and Dr. Feng Xiong (China Zebrafish Resource Center, Institute of Hydrobiology, Chinese Academy of Sciences) for assistance with qPCR analysis.

This work was supported by the Strategic Priority Research Program of the Chinese Academy of Sciences (XDB0730300), National Excellent Youth Science Fund (32322086), National Natural Science Foundation of China (32073009), and the Youth Innovation Promotion Association provided funding to Shun Li. National Key Research and Development Program of China (2023YFD2400201) provided funding to Dan-Dan Chen. National Natural Science Foundation of China (32173023) provided funding to Long-Feng Lu.

Author Contributions

L.F.L. and S.L. conceptualized the study and wrote the original draft. L.F.L. did data analysis. C.Z., Z.C.L., and B.J.C. were responsible for sample collection. D.D.C., S.L., and L.F.L. are responsible for funding resources. All authors reviewed and edited the manuscript. All authors had full access to all the data in the study and had final responsibility for the decision to submit for publication.

Declaration of interests

The authors declare no competing interests.

References:

1. Kisseleva T, Bhattacharya S, Braunstein J, Schindler CW. Signaling through the JAK/STAT pathway, recent advances and future challenges. *Gene* **285**, 1-24 (2002).

2. Sadler AJ, Williams BRG. Interferon-inducible antiviral effectors. *Nat Rev Immunol* **8**, 559-568 (2008).

3. Kumar H, Kawai T, Akira S. Pathogen recognition by the innate immune system. *Int Rev Immunol* **30**, 16-34 (2011).

4. Fitzgerald KA, *et al*. IKKepsilon and TBK1 are essential components of the IRF3 signaling

pathway. *Nat Immunol* **4**, 491-496 (2003).

5. Zhao W. Negative regulation of TBK1-mediated antiviral immunity. *FEBS letters* **587**, 542-548 (2013).

6. Cui J, *et al.* NLRP4 negatively regulates type I interferon signaling by targeting the kinase TBK1 for degradation via the ubiquitin ligase DTX4. *Nature immunology* **13**, 387-395 (2012).

7. Cui J, *et al.* NLRP4 negatively regulates type I interferon signaling by targeting the kinase TBK1 for degradation via the ubiquitin ligase DTX4. *Nat Immunol* **13**, 387-395 (2012).

8. An T, *et al.* DYRK2 Negatively Regulates Type I Interferon Induction by Promoting TBK1 Degradation via Ser527 Phosphorylation. *PLoS pathogens* **11**, e1005179 (2015).

9. Lu LF, *et al.* A novel role of Zebrafish TMEM33 in negative regulation of interferon production by two distinct mechanisms. *PLoS pathogens* **17**, e1009317 (2021).

10. Fagundes R, Teixeira LK. Cyclin E/CDK2: DNA Replication, Replication Stress and Genomic Instability. *Front Cell Dev Biol* **9**, (2021).

11. Schmitz ML, Kracht M. Cyclin-Dependent Kinases as Coregulators of Inflammatory Gene Expression. *Trends Pharmacol Sci* **37**, 101-113 (2016).

12. Chen Y, *et al.* CDK2 Inhibition Enhances Antitumor Immunity by Increasing IFN Response to Endogenous Retroviruses. *Cancer Immunol Res* **10**, 525-539 (2022).

13. Cingoz O, Goff SP. Cyclin-dependent kinase activity is required for type I interferon production. *Proc Natl Acad Sci U S A* **115**, E2950-E2959 (2018).

14. Sun F, *et al.* Characterization of fish IRF3 as an IFN-Iinducible protein reveals evolving regulation of IFN response in vertebrates. *J Immunol* **185**, 7573-7582 (2010).

15. Panne D, McWhirter SM, Maniatis T, Harrison SC. Interferon regulatory factor 3 is regulated by a dual phosphorylation-dependent switch. *J Biol Chem* **282**, 22816-22822 (2007).

16. Li S, *et al.* Zebrafish MVP Recruits and Degrades TBK1 To Suppress IFN Production. *The Journal of Immunology* **202**, 559-566 (2019).

17. Liu S, *et al.* Major vault protein: A virus-induced host factor against viral replication through the induction of type-I interferon. *Hepatology* **56**, 57-66 (2012).

18. Wu SY, *et al.* HER2 recruits AKT1 to disrupt STING signalling and suppress antiviral defence and antitumour immunity. *Nature cell biology* **21**, 1027-+ (2019).

19. Zheng Q, Hou J, Zhou Y, Yang Y, Xie B, Cao X. Siglec1 suppresses antiviral innate immune response by inducing TBK1 degradation via the ubiquitin ligase TRIM27. *Cell research* **25**, 1121-1136 (2015).

20. Yan XL, Zheng WW, Geng S, Zhou M, Xu TJ. Cytokine Receptor-Like Factor 3 Negatively Regulates Antiviral Immunity by Promoting the Degradation of TBK1 in Teleost Fish. *Journal of virology* **97**, (2023).

21. Song L, Luo ZQ. Post-translational regulation of ubiquitin signaling. *The Journal of cell biology* **218**, 1776-1786 (2019).

22. Kulathu Y, Komander D. Atypical ubiquitylation - the unexplored world of polyubiquitin beyond Lys48 and Lys63 linkages. *Nat Rev Mol Cell Biol* **13**, 508-523 (2012).

23. Wang C, *et al*. The E3 ubiquitin ligase Nrdp1 'preferentially' promotes TLR-mediated production of type I interferon. *Nature immunology* **10**, 744-752 (2009).

24. Ye JS, Kim N, Lee KJ, Nam YR, Lee U, Joo CH. Lysine 63-Linked TANK-Binding Kinase 1 Ubiquitination by Mindbomb E3 Ubiquitin Protein Ligase 2 Is Mediated by the Mitochondrial Antiviral Signaling Protein. *Journal of virology* **88**, 12765-12776 (2014).

25. Song GH, *et al*. E3 ubiquitin ligase RNF128 promotes innate antiviral immunity through K63-linked ubiquitination of TBK1. *Nature immunology* **17**, 1342-1351 (2016).

26. Zhang R, Yang W, Zhu H, Jingbo Z, Xue M, Zheng C. NLRC4 promotes the cGAS-STING signaling pathway by facilitating CBL-mediated K63-linked polyubiquitination of TBK1. *Journal of medical virology* **95**, e29013 (2023).

27. Zhang M, *et al*. TRAF-interacting protein (TRIP) negatively regulates IFN-beta production and antiviral response by promoting proteasomal degradation of TANK-binding kinase 1. *The Journal of experimental medicine* **209**, 1703-1711 (2012).

28. Liu D, *et al*. SOCS3 Drives Proteasomal Degradation of TBK1 and Negatively Regulates Antiviral Innate Immunity. *Molecular and cellular biology* **35**, 2400-2413 (2015).

29. Deng M, *et al*. TRAF3IP3 negatively regulates cytosolic RNA induced anti-viral signaling by promoting TBK1 K48 ubiquitination. *Nat Commun* **11**, 2193 (2020).

30. Friedman CS, *et al*. The tumour suppressor CYLD is a negative regulator of RIG-I-mediated antiviral response. *EMBO reports* **9**, 930-936 (2008).

31. Zhang Z, *et al*. RNF144B inhibits LPS-induced inflammatory responses via binding TBK1. *J Leukoc Biol* **106**, 1303-1311 (2019).

32. Zhang L, Zhao X, Zhang M, Zhao W, Gao C. Ubiquitin-specific protease 2b negatively regulates IFN-beta production and antiviral activity by targeting TANK-binding kinase 1. *Journal of immunology* **193**, 2230-2237 (2014).

33. Huang L, *et al*. Ubiquitin-Conjugating Enzyme 2S Enhances Viral Replication by Inhibiting Type I IFN Production through Recruiting USP15 to Deubiquitinate TBK1. *Cell reports* **32**, (2020).

34. Yu Z, *et al*. USP1–UAF1 deubiquitinase complex stabilizes TBK1 and enhances antiviral responses. *The Journal of experimental medicine* **214**, jem.20170180 (2017).

35. Pickart CM. Mechanisms underlying ubiquitination. *Annu Rev Biochem* **70**, 503-533 (2001).

36. Metzger MB, Hristova VA, Weissman AM. HECT and RING finger families of E3 ubiquitin ligases at a glance. *Journal of cell science* **125**, 531-537 (2012).

37. Cui J, *et al*. NLRP4 negatively regulates type I interferon signaling by targeting the kinase TBK1 for degradation via the ubiquitin ligase DTX4. *Nature immunology* **13**, 387-395 (2012).

38. Zheng CF, Tang YD. The emerging roles of the CDK/cyclin complexes in antiviral innate immunity. *Journal of Medical Virology* **94**, 2384-2387 (2022).

39. Yamamoto S, *et al*. Mediator cyclin-dependent kinases upregulate transcription of inflammatory genes in cooperation with NF-B and C/EBP on stimulation of Toll-like receptor 9. *Genes Cells* **22**, 265-276 (2017).

40. Perkins ND, Felzien LK, Betts JC, Leung KY, Beach DH, Nabel GJ. Regulation of NF-kappa B by cyclin-dependent kinases associated with the p300 coactivator. *Science* **275**, 523-527 (1997).

41. Wu LL, *et al*. Identification of Cyclin-Dependent Kinase 1 as a Novel Regulator of Type I Interferon Signaling in Systemic Lupus Erythematosus. *Arthritis Rheumatol* **68**, 1222-1232 (2016).

42. Cingöz O, Goff SP. Cyclin-dependent kinase activity is required for type I interferon production. *P Natl Acad Sci USA* **115**, E2950-E2959 (2018).

43. Tadesse S, *et al*. Targeting CDK2 in cancer: challenges and opportunities for therapy. *Drug Discov Today* **25**, 406-413 (2020).

44. Hirai T, *et al*. Isolation and Characterization of Goldfish Cdk2, a Cognate Variant of the Cell-Cycle Regulator Cdc2. *Developmental biology* **152**, 113-120 (1992).

45. Chu J, *et al*. UHRF1 phosphorylation by cyclin A2/cyclin-dependent kinase 2 is required for zebrafish embryogenesis. *Molecular biology of the cell* **23**, 59-70 (2012).

46. Xu Y, Tian Y, Zhao H, Zheng N, Ren KX, Li QW. A novel CDK-2 homolog identified in lamprey, with roles in apoptosis. *Fish Physiol Biochem* **47**, 189-189 (2021).

47. Mai WJ, Liu HX, Chen HQ, Zhou YJ, Chen Y. RGNNV-induced cell cycle arrest at G1/S phase enhanced viral replication via p53-dependent pathway in GS cells. *Virus Res* **256**, 142-152 (2018).

Figure Legends

Figure 1. *In vivo and in vitro*, CDK2 is upregulated during viral infection. (A) Schematic representation of zebrafish tissue dissection and RNA extraction for transcriptome sequencing. The liver and spleen tissues from male and female zebrafish injected with PBS (5 μL/individual), SVCV (5 × 10^8 $TCID_{50}$/mL, 5 μL/individual) for 48 h. Total RNAs were extracted and used for transcriptome sequencing and analysis. (B) Heatmap view of mRNA variations of CDKs in the liver and spleen of zebrafish with or without SVCV infection. (C) qPCR analysis of *cdk2* mRNA in the THP-1, GICB, ZF4, or EPC cells infected with VSV, CyHV-2, or SVCV for the indicated times. (D) qPCR analysis of *cdk2* mRNA in the liver and spleen of zebrafish (n = 5 per group) given injected intraperitoneally (i.p.) with PBS or SVCV for 48 h. (E) IB of proteins in the liver and spleen of zebrafish (n = 3 per group) given i.p. injection of PBS or SVCV for 48 h. (F) IB of proteins in ZF4 and EPC cells infected with SVCV for the indicated times.

Figure 2. CDK2 deficiency protects fish from SVCV infection. (A) Survival (Kaplan-Meier Curve) of *cdk2*$^{+/+}$ and *cdk2*$^{-/-}$ zebrafish (n = 15 per group) at various days after i.p. infected with SVCV (5 × 10^8 $TCID_{50}$/mL, 5 μL/individual). (B) Microscopy of H&E-stained liver, spleen, and kidney sections from *cdk2*$^{+/+}$ and *cdk2*$^{-/-}$ zebrafish treated with SVCV for 48 h. (C) qPCR analysis of *svcv-n* mRNA in the liver, spleen, and kidney of *cdk2*$^{+/+}$ and *cdk2*$^{-/-}$ zebrafish (n = 6 per group) given i.p.

injection of SVCV for 48 h. (D) IB of proteins in the liver, spleen, and kidney sections from *cdk2*$^{+/+}$ and *cdk2*$^{-/-}$ zebrafish (n = 3 per group) treated with SVCV for 48 h. (E) CDK2 regulates antiviral response-relevant target genes, presented as a volcano plot of genes with differential expression after SVCV infection in the liver of *cdk2*$^{+/+}$ and *cdk2*$^{-/-}$ zebrafish. (F) GSEA of differentially expressed genes in the liver of *cdk2*$^{+/+}$ and *cdk2*$^{-/-}$ zebrafish with SVCV infection and enrichment of IFN. FDR (*q*-value) was shown. (G) Heatmap view of mRNA variations of IFN-mediated ISG sets in the liver of *cdk2*$^{+/+}$ and *cdk2*$^{-/-}$ zebrafish with SVCV infection. (H) qPCR analysis of *ifnφ1* mRNA in the liver, spleen, and kidney of *cdk2*$^{+/+}$ and *cdk2*$^{-/-}$ zebrafish (n = 6 per group) given i.p. injection of SVCV for 48 h.

Figure 3. CDK2 negatively regulates IFN production and promotes viral replication. (A and C) Luciferase activity of IFNφ1pro and ISRE in EPC cells transfected with indicated plasmids for 24 h, and then untreated or infected with SVCV (MOI = 1) or transfected with poly I:C (0.5 μg) for 24 h before luciferase assays. (B) IB of proteins in EPC cells transfected with indicated plasmids for 24 h. (D) qPCR analysis of *ifn* and *vig1* in EPC cells transfected with indicated plasmids for 24 h, and then untreated or infected with SVCV (MOI = 1) or transfected with poly I:C (2 μg) for 24 h. (E and F) Plaque assay of virus titers in EPC, CIK, and GiCB cells transfected with indicated plasmids for 24 h, followed by SVCV, GCRV, and CyHV-2 challenge for 24-72 h. (G and H) qPCR and IB analysis of SVCV genes in EPC cells transfected with indicated plasmids for 24 h, followed by SVCV challenge for 24 h. (I) IF analysis of N protein in EPC cells transfected with indicated plasmids for 24 h, followed by SVCV challenge for 24 h. The fluorescence intensity (arbitrary unit, a.u.) was recorded by the LAS X software, and the data were expressed as mean ± SD, n = 5.

Figure 4. CDK2 associates with TBK1 and mediates its degradation. (A and B) Luciferase activity of IFNφ1pro and ISRE in EPC cells transfected with indicated plasmids for 24 h. (C and D) qPCR analysis of *ifn* and *vig1* in EPC cells transfected with indicated plasmids for 24 h. (E) Confocal microscopy of CDK2 and TBK1 in EPC cells transfected with indicated plasmids for 24 h. The coefficient of

colocalization was determined by qualitative analysis of the fluorescence intensity of the selected area in Merge. (F) IB of WCLs and proteins immunoprecipitated with anti-Myc antibody-conjugated agarose beads from EPC cells transfected with indicated plasmids for 24 h. (G) IB of WCLs and proteins immunoprecipitated with anti-TBK1 or anti-CDK2 antibody from EPC cells infected with SVCV for 24 h. (H) Schematic representation of full-length TBK1 and its mutants. (I) IB of WCLs and proteins immunoprecipitated with anti-Flag antibody-conjugated agarose beads from EPC cells transfected with indicated plasmids for 24 h. (J) IB of proteins in EPC cells transfected with indicated plasmids for 24 h. (K and L) IB of proteins in EPC cells transfected with CDK2-HA or sh*cdk2*#1 for 24 h, followed by untreated or infected with SVCV (MOI = 1) or transfected with poly I:C (2 μg) for 24 h. (M) IB of proteins in the liver, spleen, and kidney sections from *cdk2*$^{+/+}$ and *cdk2*$^{-/-}$ zebrafish (n = 3 per group). (N) Plaque assay of virus titers in EPC cells transfected with indicated plasmids for 24 h, followed by SVCV challenge for 24-48 h. (O and Q) IB and qPCR analysis of SVCV genes in EPC cells transfected with indicated plasmids for 24 h, followed by SVCV challenge for 24 h. (P) IF analysis of N protein in EPC cells transfected with indicated plasmids for 24 h, followed by SVCV challenge for 24 h. The fluorescence intensity (arbitrary unit, a.u.) was recorded by the LAS X software, and the data were expressed as mean ± SD, n = 5.

Figure 5. CDK2 increases the K48-linked polyubiquitination of TBK1. (A) qPCR analysis of *epc-tbk1* in EPC cells transfected with indicated plasmids for 24 h, and then untreated or infected with SVCV (MOI = 1) or transfected with poly I:C (2 μg) for 24 h. (B and C) IB of proteins in EPC cells transfected with indicated plasmids for 18 h, followed by treatments of MG132 (10 μM), 3-MA (2 mM), Baf-A1 (100 nM), and CQ (50 μM) for 6 h, respectively. (D) IB of proteins in EPC cells transfected with CDK2-HA for 24 h, followed by untreated or infected with SVCV (MOI = 1) or transfected with poly I:C (2 μg) for 24 h. Protein lysates were harvested after MG132 (20 μM) treatments (6 h) for IB analysis. (E) TBK1 ubiquitination assays in EPC cells transfected with indicated plasmids for 18 h, followed by DMSO or MG132 treatments for 6 h. (F) Mass spectrometry analysis of a peptide derived from

879 ubiquitinated TBK1-Myc. (G and H) TBK1 ubiquitination assays in EPC cells
880 transfected with indicated plasmids for 18 h, followed by MG132 treatments for 6 h.
881 **Figure 6. CDK2 recruits Dtx4 to degrade TBK1.** (A-D) IB of WCLs and proteins
882 immunoprecipitated with anti-Myc or Flag Ab-conjugated agarose beads from EPC
883 cells transfected with indicated plasmids for 24 h. (E and J) Luciferase activity of
884 IFNφ1pro in EPC cells transfected with indicated plasmids for 24 h. (F and K) qPCR
885 analysis of *ifn* and *vig1* in EPC cells transfected with indicated plasmids for 24 h. (G
886 and L) IB of proteins in EPC cells transfected with indicated plasmids for 24 h. (H
887 and M) IB of proteins in EPC cells transfected with CDK2-HA and Dtx4-Myc or
888 sh*dtx4*#1 for 24 h, followed by untreated or infected with SVCV (MOI = 1) or
889 transfected with poly I:C (2 μg) for 24 h.
890 **Figure 7. K567 site is critical for the ubiquitination degradation of TBK1.** (A-C)
891 TBK1 ubiquitination assays in EPC cells transfected with indicated plasmids for 18 h,
892 followed by MG132 treatments for 6 h. (D) Mass spectrometry analysis to show that
893 K154 and K567 of TBK1 is conjugated with ubiquitin. (E-H) TBK1 ubiquitination
894 assays in EPC cells transfected with indicated plasmids for 18 h, followed by MG132
895 treatments for 6 h. (I) IB of proteins in EPC cells transfected with indicated plasmids
896 for 24 h. (J) Luciferase activity of IFNφ1pro in EPC cells transfected with indicated
897 plasmids for 24 h. (K) qPCR analysis of *ifn* in EPC cells transfected with indicated
898 plasmids for 24 h. (L) Plaque assay of virus titers in EPC cells transfected with
899 indicated plasmids for 24 h, followed by SVCV challenge for 24-48 h. (M and N)
900 qPCR and IB analysis of SVCV genes in EPC cells transfected with indicated
901 plasmids for 24 h, followed by SVCV challenge for 24 h. (O) IF analysis of N protein
902 in EPC cells transfected with indicated plasmids for 24 h, followed by SVCV
903 challenge for 24 h. The fluorescence intensity (arbitrary unit, a.u.) was recorded by
904 the LAS X software, and the data were expressed as mean ± SD, n = 5. (P) Schematic
905 representation of full-length Dtx4 and its mutants. (Q) IB of WCLs and proteins
906 immunoprecipitated with anti-Myc or HA Ab-conjugated agarose beads from EPC
907 cells transfected with indicated plasmids for 24 h. (R) TBK1 ubiquitination assays in
908 EPC cells transfected with indicated plasmids for 18 h, followed by MG132

909 treatments for 6 h.

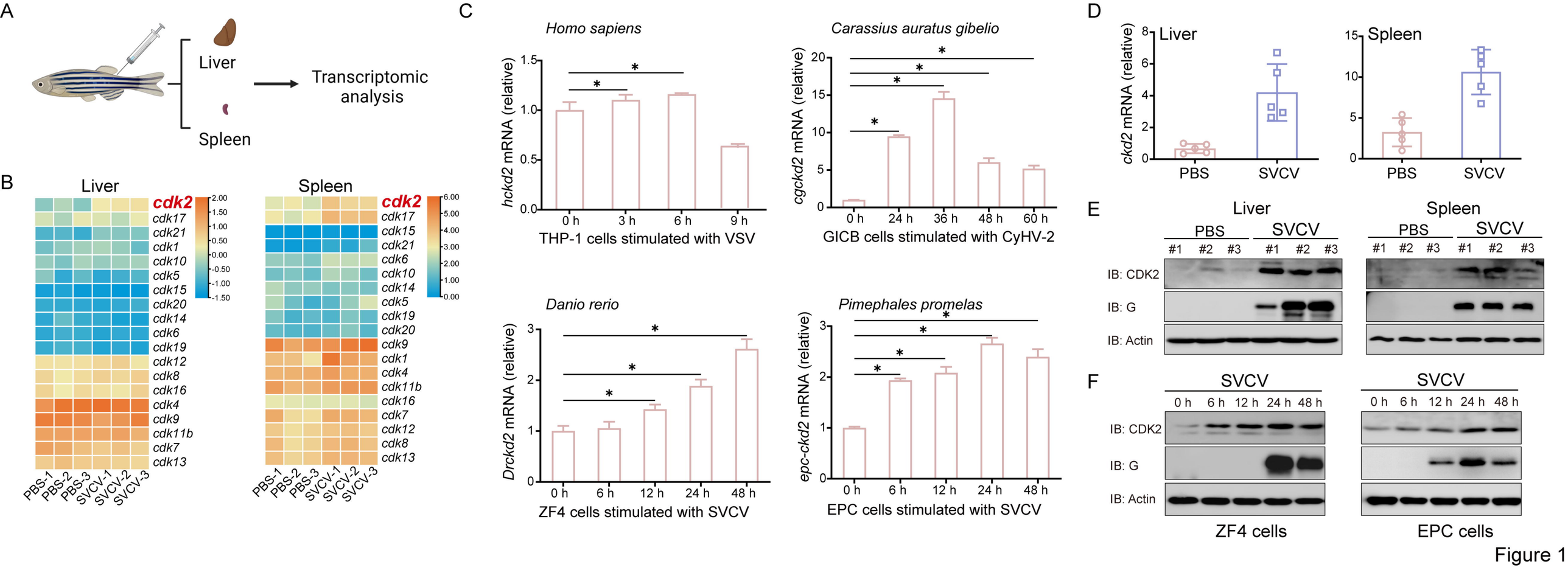
A
Liver
Spleen
Transcriptomic analysis
B
Liver
Spleen
cdk2
cdk17
cdk21
cdk1
cdk10
cdk5
cdk15
cdk20
cdk14
cdk6
cdk19
cdk12
cdk8
cdk16
cdk4
cdk9
cdk11b
cdk7
cdk13
PBS-1
PBS-2
PBS-3
SVCV-1
SVCV-2
SVCV-3
C
Homo sapiens
hckd2 mRNA (relative)
THP-1 cells stimulated with VSV
Carassius auratus gibelio
cgckd2 mRNA (relative)
GICB cells stimulated with CyHV-2
Danio rerio
Drckd2 mRNA (relative)
ZF4 cells stimulated with SVCV
Pimephales promelas
epc-ckd2 mRNA (relative)
EPC cells stimulated with SVCV
D
Liver
Spleen
ckd2 mRNA (relative)
PBS
SVCV
E
Liver
Spleen
IB: CDK2
IB: G
IB: Actin
F
SVCV
ZF4 cells
EPC cells

Figure 1

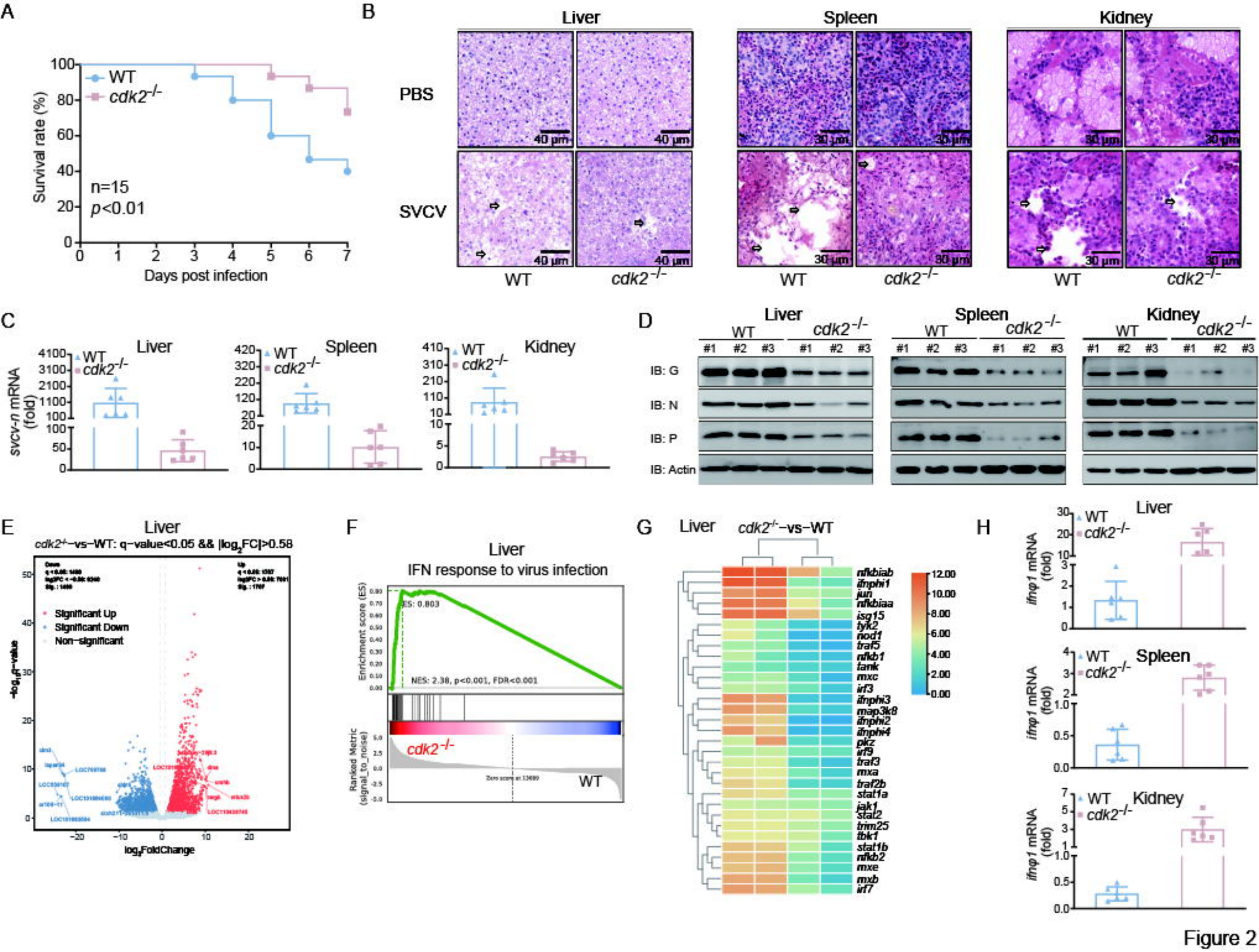
A
Survival rate (%)
Days post infection
WT
cdk2-/-
n=15
p<0.01
B
Liver
Spleen
Kidney
PBS
SVCV
WT
cdk2-/-
40 μm
30 μm
C
svcv-n mRNA (fold)
Liver
Spleen
Kidney
D
IB: G
IB: N
IB: P
IB: Actin
#1 #2 #3
E
Liver
cdk2-/- vs WT: q-value<0.05 && |log2FC|>0.58
Significant Up
Significant Down
Non-significant
-log10q-value
log2FoldChange
F
Liver
IFN response to virus infection
Enrichment score (ES)
ES: 0.803
NES: 2.38, p<0.001, FDR<0.001
Ranked Metric (signal_to_noise)
cdk2-/-
WT
G
Liver
cdk2-/- vs WT
nfkbiab
ifnphi1
jun
nfkbiaa
isg15
tyk2
nod1
traf5
nfkb1
tank
mxc
irf3
ifnphi3
map3k8
ifnphi2
ifnphi4
pkz
irf9
traf3
mxa
traf2b
stat1a
jak1
stat2
trim25
tbk1
stat1b
nfkb2
mxe
mxb
irf7
H
ifnφ1 mRNA (fold)
Liver
Spleen
Kidney

Figure 2

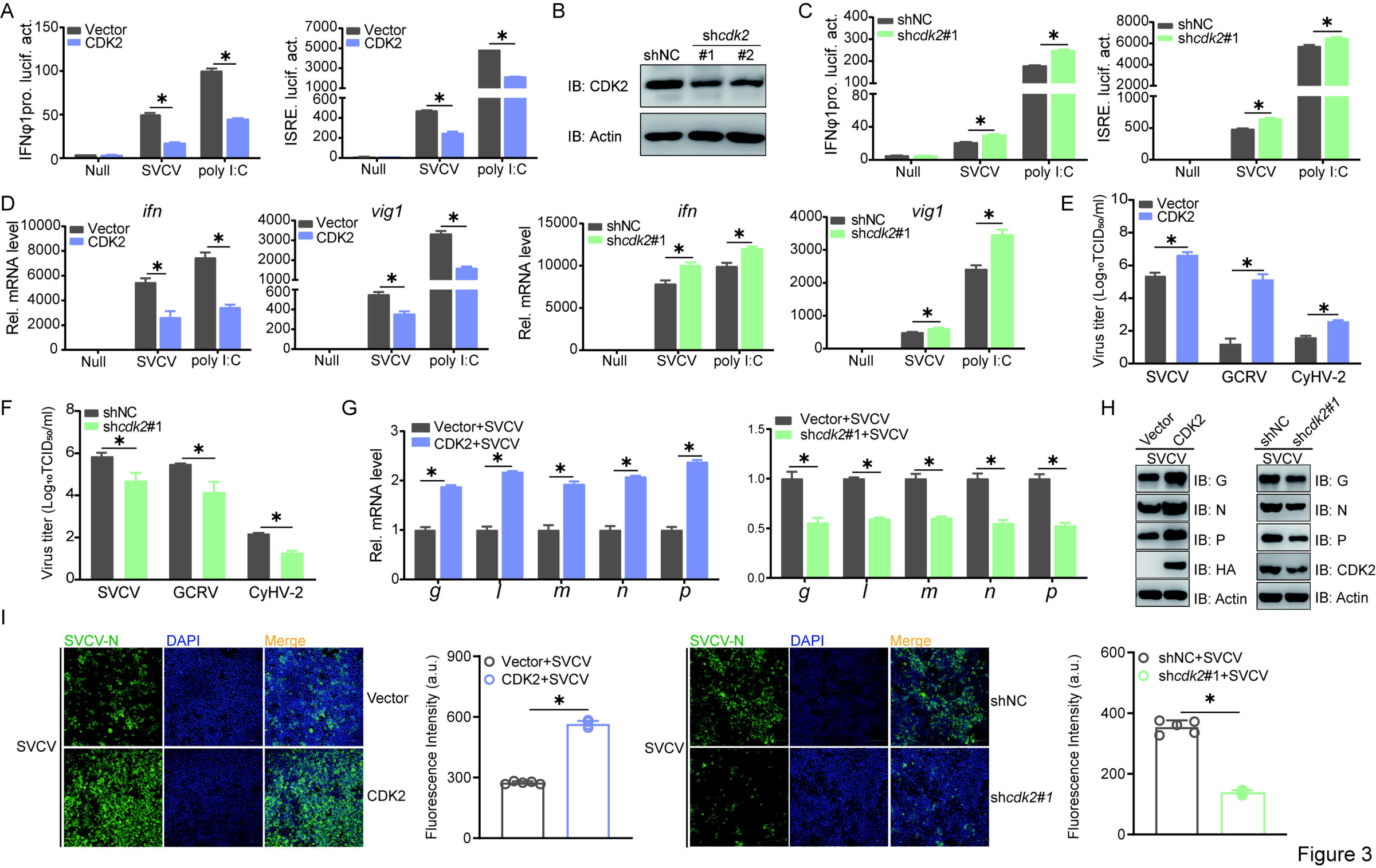
A
IFNφ1pro. lucif. act.
Vector
CDK2
Null
SVCV
poly I:C
ISRE. lucif. act.
B
shcdk2
shNC
#1
#2
IB: CDK2
IB: Actin
C
shNC
shcdk2#1
D
ifn
vig1
Rel. mRNA level
E
Virus titer (Log10TCID50/ml)
SVCV
GCRV
CyHV-2
F
G
Vector+SVCV
CDK2+SVCV
shcdk2#1+SVCV
g
l
m
n
p
H
IB: G
IB: N
IB: P
IB: HA
IB: CDK2
IB: Actin
I
SVCV-N
DAPI
Merge
Fluorescence Intensity (a.u.)

Figure 3

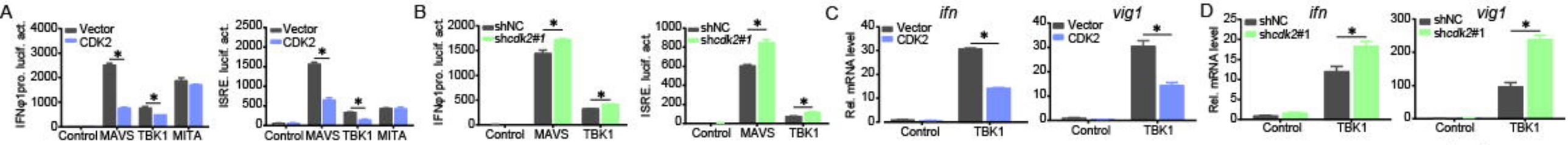
A
IFNφ1pro. lucif. act.
Vector
CDK2
Control MAVS TBK1 MITA
ISRE. lucif. act.
B
shNC
shcdk2#1
C
ifn
vig1
Rel. mRNA level
D
E
CDK2-GFP
MAVS-mCherry
TBK1-mCherry
Merge
Green (CDK2)
Red (TBK1)
Fluorescent Intensity
Distance (pixels)
F
Vector
MAVS-Myc
TBK1-Myc
CDK2-HA
IP: Myc
IB: HA
IB: Myc
WCL
G
SVCV
IP: IgG αTBK1
IP: IgG αCDK2
IB: CDK2
IB: TBK1
H
TBK1
TBK1ΔN
TBK1ΔC
Idnase domain
CCD
I
CDK2-Myc
IP: Flag
WCL
TBK1-Flag
TBK1-ΔN-Flag
TBK1-ΔC-Flag
TBK1
TBK1-ΔN
TBK1-ΔC

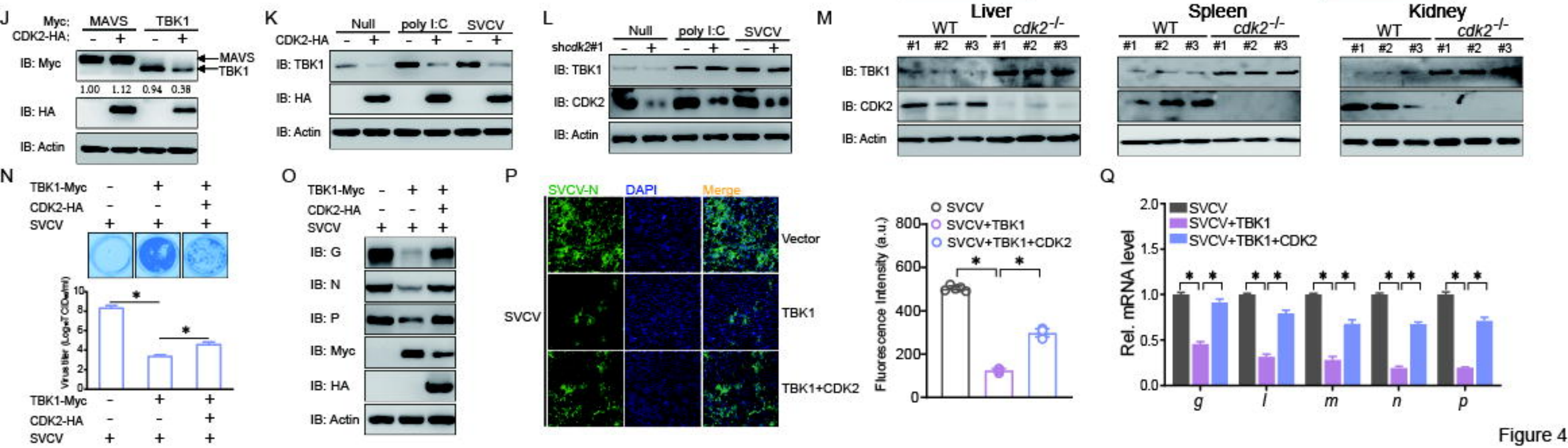
J
Myc:
CDK2-HA:
MAVS
TBK1
IB: Myc
IB: HA
IB: Actin
1.00 1.12 0.94 0.38
K
Null
poly I:C
SVCV
L
shcdk2#1
M
Liver
Spleen
Kidney
WT
cdk2-/-
N
TBK1-Myc
CDK2-HA
SVCV
Virus titer (Log₁₀TCID₅₀/ml)
O
IB: G
IB: N
IB: P
P
SVCV-N
DAPI
Merge
Vector
TBK1
TBK1+CDK2
Fluorescence Intensity (a.u.)
SVCV
SVCV+TBK1
SVCV+TBK1+CDK2
Q
Rel. mRNA level
g
l
m
n
p

Figure 4

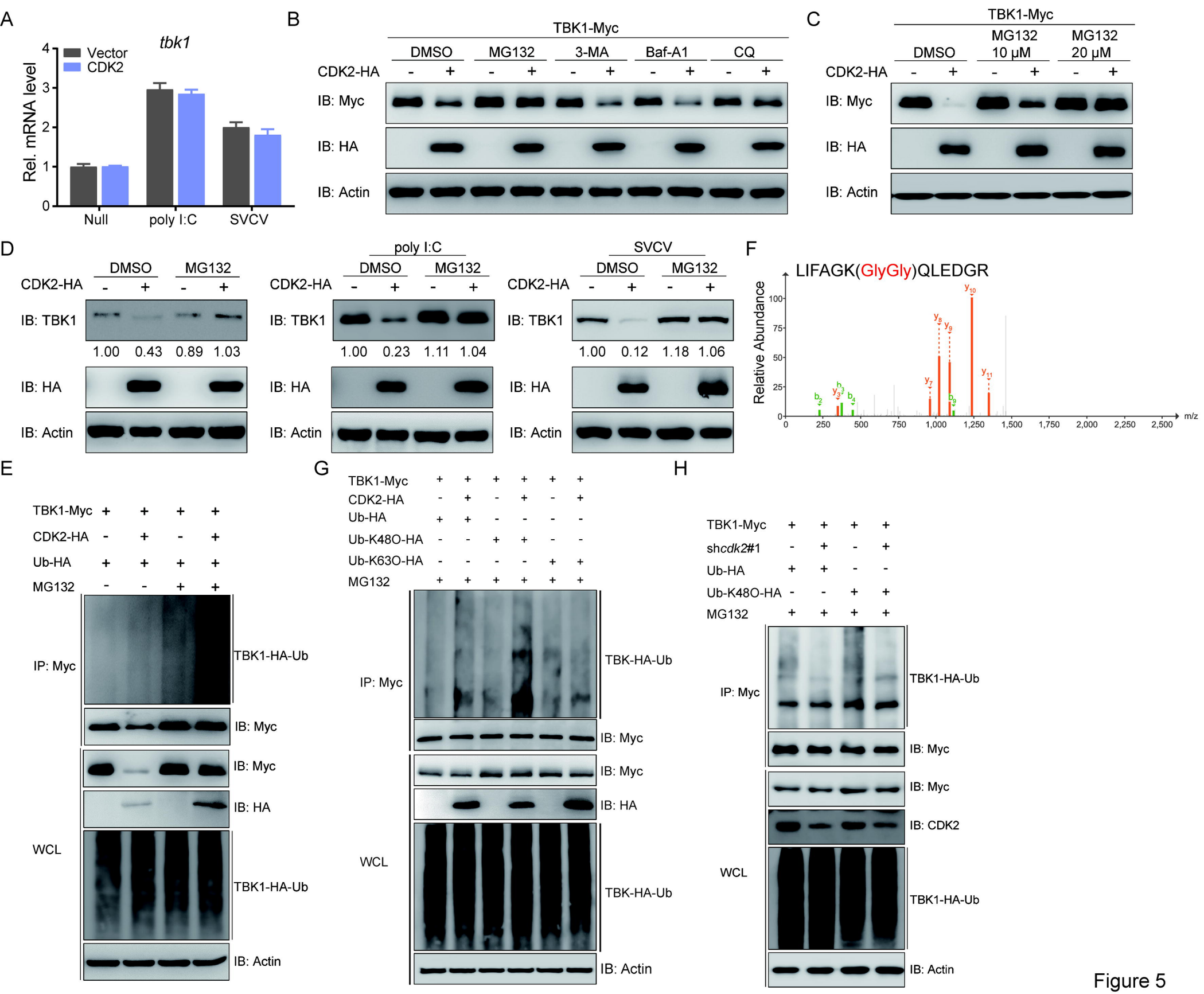
A
tbk1
Vector
CDK2
Rel. mRNA level
Null
poly I:C
SVCV
B
TBK1-Myc
DMSO
MG132
3-MA
Baf-A1
CQ
CDK2-HA
IB: Myc
IB: HA
IB: Actin
C
TBK1-Myc
DMSO
MG132 10 μM
MG132 20 μM
CDK2-HA
IB: Myc
IB: HA
IB: Actin
D
poly I:C
SVCV
DMSO
MG132
CDK2-HA
IB: TBK1
1.00 0.43 0.89 1.03
1.00 0.23 1.11 1.04
1.00 0.12 1.18 1.06
IB: HA
IB: Actin
F
LIFAGK(GlyGly)QLEDGR
Relative Abundance
m/z
E
TBK1-Myc
CDK2-HA
Ub-HA
MG132
IP: Myc
TBK1-HA-Ub
IB: Myc
IB: HA
WCL
IB: Actin
G
TBK1-Myc
CDK2-HA
Ub-HA
Ub-K48O-HA
Ub-K63O-HA
MG132
IP: Myc
TBK-HA-Ub
IB: Myc
IB: HA
WCL
IB: Actin
H
TBK1-Myc
shcdk2#1
Ub-HA
Ub-K48O-HA
MG132
IP: Myc
TBK1-HA-Ub
IB: Myc
IB: CDK2
WCL
IB: Actin

Figure 5

Figure 6

Figure 7